Applied Radiation and Isotopes 206 (2024) 111193

Contents lists available at ScienceDirect

Applied Radiation and Isotopes

journal homepage: www.elsevier.com/locate/apradiso

Relativistic impulse approximation-based compton component of mass energy absorption coefficients (cm^2/g) for few materials of medical interest

V Rao Donepudi [a,*], E Gigante Giovanni [a], Tetsuya Yusa [b], Tako Akatsuka [b], Tohoru Takeda [c], Roberto Cesareo [d], Antonio Brunetti [d], Nick Schiavon [e]

[a] Department of Science Based Applications to Engineering (SBAI), Physics Division, University of Rome "La Sapienza" Via Scarpa 10, 00161, Roma, Italy
[b] Department of Bio-System Engineering, Faculty of Engineering, Yamagata University, Yonezawa, Japan
[c] Health Science Division, Kitasato University, Kitasato, Japan
[d] Instituto di Fisica e Mathematica, Universita di Sassari, Via Vienna, Sassari, 2-07100, Italy
[e] Hercules Laboratory, University of Evora, Portugal

A R T I C L E I N F O

Keywords:
Relativistic
Impulse approximation
Compton
Total cross section
Integrated cross section
Photon transport
Energy absorption and biological materials

A B S T R A C T

Total, whole-atom, individual and integrated Compton scattering cross sections and Compton energy absorption scattering cross sections are evaluated for light elements, such as, H, C, N, O, P, and Ca, with relativistic impulse approximation methods. Most of the phantom materials composed of these elements, which are the basic constituents of biological soft-tissue and attenuation through them, provides potential source of information. Compton scattering cross-sections for few biological materials, such as, H_2O, C_2H_4, C_8H_8, $C_5H_8O_2$, $C_6H_{11}NO$, $C_{16}H_{14}O_3$, $C_{55}H_{102}O_6$, $[Ca_3(PO_4)]_3Ca\ (OH)_2$ of medical interest, have been evaluated with the use of double differential scattering cross-section based on impulse approximation. Utilized these values to evaluate the Compton energy absorption cross sections and Compton component of mass energy absorption coefficients (cm^2/g) in the energy region from 0.005 to 10 MeV. The derived results are compared with the theoretical tabulations.

1. Introduction

Compton scattering cross-sections, energy absorption cross sections and the Compton component of the mass energy absorption coefficient are extensively used in the field of radiological sciences (Hubbell et al., 1975; Hubbell, 1977; Hubbell, 1982; Cesareo et al., 1992; Hubbell, 1999; Hubbell, 2006). One particular area of interest is in Monte Carlo simulation of photon transport in applications of medical physics (Boone and Chavez, 1996). In other fields such as nuclear power plant shielding, health physics and industrial irradiation and monitoring, and in x-ray crystallography. In dosimetry calculations, use is frequently made of the Compton energy absorption cross section per electron (σ_{en}), which expresses the probability of transfer of energy from a photon to an electron by the Compton process. It is equal to the total Compton scattering cross section per electron (σ_{TC}) times the fraction (f) of photon energy, which is converted to kinetic energy of the recoil electrons in a single collision, averaged over all directions of electron recoil ($\sigma_{en} = \sigma_{TC}$ x f). Since the range of the recoil electron is small, the Compton energy absorption cross section per electron is a measure of the total energy communicated locally to the absorbing medium by the Compton process (Seltzer, 1993; Rao et al., 2002a,b). Majority of the light elements, such as, H, C, N, O, and P, constitute the soft-tissue. Double differential scattering cross sections are evaluated for the above light elements. Utilized these values to derive the Compton energy absorption cross sections and Compton component of mass energy absorption coefficients (cm^2/g) in the energy region from 0.005 to 10 MeV (Rao, 2000; Rao et al. 2003; Rao et al., 2004a,b). The mass attenuation coefficient in which the dependence on the density has been removed. It can be obtained as the sum of the different types of possible interactions of photons with atoms of the material (Rao et al., 2002a, b; 2007). These papers covers, energy and geometrical broadening, FWHM of J (p_z) and FWHM of Compton broadening, estimated for a number of Kα x-ray energies and for 59.64 keV(Am-241) γ-photons. The interaction of photons below 1 MeV, through various processes (Compton, Rayleigh and atomic photoeffect) may be interesting to know more about the fundamental radiation interactions from biological materials, many of them contain the elements of the soft tissue; the data may be used for comparison and compilation purposes. Also covered the, Compton component of the mass-energy absorption coefficient, derived for individual elements and overall momentum resolution for experimental interest. Further estimated the

* Corresponding author.
E-mail address: done9venkat53@rediffmail.com (V.R. Donepudi).

https://doi.org/10.1016/j.apradiso.2024.111193
Received 10 November 2022; Received in revised form 23 July 2023; Accepted 16 January 2024
Available online 9 February 2024

Table 1
Name of the material, density and Chemical formula.

Name	ρ (g/cm^3)	Chemical formula	$N_A\rho$	M	$N_A\rho/M$
Water	1.00	H_2O	6.02E+23	18.02	33.4E+21
Nylon	1.15	$C_6H_{11}NO$	6.93E+23	113.16	6.12E+21
Polyethylene	0.92	C_2H_4	5.54E+23	28.05	19.8E+21
Lucite	1.19	$C_5H_8O_2$	7.17E+23	100.12	7.16E+21
Polystyrene	1.05	C_8H_8	6.32E+23	104.15	6.07E+21
Polycarbonate	1.20	$C_{16}H_{14}O_3$	7.23E+23	254.28	2.84E+21
Fat(Adipose tissue)	0.95	$C_{55}H_{102}O_6$	5.72E+23	859.42	0.67E+21
Bone	1.85	$H_8O_{26}P_9Ca_6$	11.1E+23	943.29	1.18E+21
Calcium hydroxyapatite	2.74	$[Ca_3(PO_4)_2]_3Ca\ (OH)_2$	16.5E+23	1004.64	1.64E+21

$N_A = 6.023 \times 1023$ atoms/mole, M = Molecular weight.

Table 2
Whole-atom Compton scattering cross-sections (b/atom) for H, C, N, O, P, and Ca in the energy region from 0.005 to 10 MeV using the tabulated values of Biggs et al. (1975).

Energy (MeV)	H	C	N	O	P	Ca
0.0050	0.4065	2.3492	2.2780	2.6514	2.7770	2.9569
0.0060	0.5078	2.4737	2.5252	2.915	3.2901	3.6127
0.0080	0.5529	2.6848	2.8836	3.3012	4.3462	4.7094
0.0100	0.5761	2.8532	3.1325	3.5708	5.0801	5.6974
0.0150	0.5965	3.1314	3.5144	3.9795	6.2281	7.4983
0.0200	0.6009	3.2744	3.7124	4.1964	6.8751	8.4583
0.0300	0.5871	3.3561	3.8522	4.3634	7.4697	9.3904
0.0400	0.5783	3.3343	3.8443	4.3700	7.6555	9.8348
0.0500	0.5515	3.2709	3.7910	4.3136	7.6642	9.8289
0.0600	0.5416	3.2056	3.7197	4.2359	7.6103	9.8827
0.0800	0.5179	3.0635	3.5621	4.0614	7.4069	9.7364
0.1000	0.4867	2.9274	3.4096	3.8907	7.1523	9.3395
0.1500	0.4542	2.6555	3.0893	3.5260	6.2755	8.7812
0.2000	0.4074	2.4332	2.8351	3.2380	6.0289	8.0117
0.3000	0.3555	2.1183	2.4693	2.8211	5.2699	7.0282
0.4000	0.3147	1.8964	2.2131	2.5291	4.7298	6.2747
0.5000	0.2903	1.7342	2.0222	2.3106	4.3266	5.7757
0.6000	0.2674	1.6036	1.8707	2.1378	4.0031	5.3347
0.8000	0.2347	1.4087	1.6434	1.8781	3.5182	4.6868
1.0000	0.2114	1.2667	1.4775	1.6885	3.1416	4.2215
1.5000	0.1714	1.0288	1.2003	1.3717	2.5712	3.4272
2.0000	0.1463	0.8776	1.0239	1.1702	2.1937	2.9237
3.0000	0.1150	0.6902	0.8052	0.9202	1.7252	2.3003
4.0000	0.0959	0.5755	0.6714	0.7674	1.4386	1.9182
5.0000	0.0828	0.4969	0.5797	0.6625	1.2422	1.6561
6.0000	0.0732	0.4391	0.5122	0.5858	1.0977	1.4637
8.0000	0.0598	0.3591	0.4189	0.4786	0.8976	1.1968
10.0000	0.0509	0.3057	0.3566	0.4076	0.7642	1.0190

Table 3
Compton energy absorption cross-sections (b/atom) for H, C, N, O, P and Ca in the energy region from 0.005 to 10 MeV using the tabulated values of Biggs et al. (1975).

Energy (MeV)	H	C	N	O	P	Ca
0.0050	0.0051	0.0243	0.0292	0.0347	0.0518	0.0560
0.0060	0.0065	0.0305	0.0362	0.0423	0.0664	0.0743
0.0080	0.0091	0.0433	0.0505	0.0583	0.0980	0.1125
0.0100	0.0115	0.0564	0.0653	0.0746	0.1252	0.1513
0.0150	0.0172	0.0889	0.1022	0.1158	0.1986	0.2474
0.0200	0.0224	0.1195	0.1376	0.1557	0.2700	0.3402
0.0300	0.0316	0.1744	0.2015	0.2282	0.4027	0.5128
0.0400	0.0394	0.2212	0.2561	0.2907	0.5203	0.6645
0.0500	0.0461	0.2610	0.3028	0.3441	0.6218	0.8011
0.0600	0.0518	0.2950	0.3426	0.3898	0.7098	0.9182
0.0800	0.0608	0.3490	0.4059	0.4624	0.8507	1.1074
0.1000	0.0675	0.3886	0.4523	0.5157	0.9547	1.2480
0.1500	0.0773	0.4467	0.5205	0.5939	1.1084	1.4574
0.2000	0.0812	0.4706	0.5486	0.6268	1.1729	1.5466
0.3000	0.0816	0.4734	0.5520	0.6304	1.1843	1.5658
0.4000	0.0782	0.4538	0.5293	0.6045	1.1372	1.5052
0.5000	0.0738	0.4286	0.4999	0.5710	1.0749	1.4237
0.6000	0.0694	0.4032	0.4703	0.5272	1.0118	1.3405
0.8000	0.0616	0.3577	0.4172	0.4766	0.8981	1.1907
1.0000	0.0552	0.3204	0.3738	0.4270	0.8049	1.0671
1.5000	0.0438	0.2543	0.2966	0.3389	0.6391	0.8474
2.0000	0.0364	0.2115	0.2468	0.2819	0.5316	0.7051
3.0000	0.0275	0.1595	0.1860	0.2126	0.4009	0.5321
4.0000	0.0221	0.1287	0.1502	0.1716	0.3236	0.4293
5.0000	0.0186	0.1083	0.1263	0.1443	0.2722	0.3614
6.0000	0.0161	0.0936	0.1092	0.1248	0.2354	0.3124
8.0000	0.0127	0.0246	0.0863	0.0986	0.1860	0.2466
10.0000	0.0105	0.0613	0.0715	0.0816	0.1541	0.2046

Compton broadening using the nonrelativistic formula for few x-ray energies and for 59.64 keV photons in the angular region 1° to 180° (Rao et al., 1999; Rao et al., 2004a,b).

It is interesting to estimate these cross sections by means of double differential scattering cross section based on impulse approximations. Impulse approximation refers to the recoil electron after momentum (Cooper, 1985). The approximation can be justified by the impulse nature of the Compton scattering process. Useful fast sampling algorithm for the simulation of Compton scattering for the unpolarised photons has developed and updated from time to time with inclusion of new computational methods (Brusa et al., 1996). Extensive experimental studies, related to inelastic x-ray and γ-ray scattering are reviewed, highlighting the importance of the data based on impulse approximation (Kane, 1997; Kane, 2006). Further, total Compton scattering cross sections and incoherent scattering factors for bound electron states of low, medim and high-Z elements have been evaluated with relativistic impulse approximation (Stutz, 2014). Earlier, widely available tabulations are non-relativistic calculations. The approaches uses, fully relativistic Klein-Nishina cross section together with a non-relativistic evaluation of incoherent scattering function. Since, many effects of the interaction of radiations with atoms depend on the so-called incoherent scattering function (Grodstein, 1957). Fully, relativistic treatment, based on impulse approximation with simple mathematical routines is useful to generate the concrete data. Scattering cross sections differential are derived in the relativistic impulse approximation for the light elements to assess the energy-broadening of Compton scattered photons. The energy broadening of the scattered photons reflects the momentum distribution of the target electrons. It increases with both increasing atomic number of the scatterer and with scattering angle (Carlsson et al., 1982; Ribberfors and Carlsson, 1985). It reflects, the evaluated double-differential cross sections, based on impulse approximation, can be used to simplify the calculations of Compton component of the mass-energy absorption coefficient. Very recently, impulse approximation-based, Compton scattering cross sections and photon attenuation coefficients used in kV dosimetry are reported. These values and the corresponding theoretical tabulations are generated with the use of python script and focused on atomic and molecular orbital calculations (Wang et al., 2020). If the electrons are in motion, as we know to be the case, there is a Doppler effect related to the projected velocities of the electrons. Relativistic impulse approximation based double differential scattering cross section includes binding effects and Doppler broadening. It leads to corrections to mass energy-absorption

Table 4
Whole-atom total Compton scattering cross-sections (b/atom) for the biological materials in the energy region from 0.005 to 10 MeV using the tabulated values of Biggs et al. (1975).

Energy (MeV)	H_2O	$C_6H_{11}NO$	C_2H_4	$C_5H_8O_2$	C_8H_8	$C_{16}H_{14}O_3$	$C_{55}H_{102}O_6$	$H_8O_{26}P_9CA_6$	$[Ca_3(PO_4)_2]_3$ $Ca(OH)_2$
0.005	3.4644	23.4961	6.3244	20.3008	22.0456	51.2324	186.5774	114.9228	115.9804
0.006	3.9306	25.8682	6.9786	22.2609	23.852	55.4334	205.3391	131.1395	132.6732
0.008	4.4070	28.3755	7.5812	24.4496	25.9016	60.601	223.867	157.6266	160.1082
0.01	4.7203	30.1596	8.0108	26.0164	27.4344	64.429	237.113	177.3549	181.4476
0.015	5.1725	32.8438	8.6488	28.388	29.8232	70.3919	256.947	209.2817	217.0116
0.02	5.3982	34.1651	8.9524	29.572	31.0024	73.3922	266.5622	226.5393	236.1418
0.03	5.5376	34.8103	9.0606	30.2041	31.5456	75.0072	270.6501	241.7149	253.3448
0.04	5.5266	34.5814	8.9818	30.0379	31.3008	74.555	268.5931	246.1547	259.0576
0.05	5.4166	33.7965	8.7478	29.3937	30.5792	72.9962	262.0341	244.5168	257.5308
0.06	5.3191	33.1468	8.5776	28.8326	29.9776	71.5797	256.9666	242.2551	255.7054
0.08	5.0972	31.7014	8.1986	27.5835	28.6512	68.4508	245.6867	234.8201	248.4376
0.1	4.8641	30.2184	7.8016	26.312	27.3128	65.3243	233.9946	225.4595	238.4404
0.15	4.4344	27.5445	7.1278	23.9631	24.8776	59.4248	213.5369	204.4763	218.0494
0.2	4.0528	25.1537	6.496	21.9012	22.7248	54.3488	194.8088	189.7775	201.2932
0.3	3.5321	21.9107	5.6586	19.0777	19.7904	47.3331	169.6941	165.7909	175.961
0.4	3.1585	19.5823	5.0516	17.0578	17.6888	42.3355	151.576	148.4906	157.5118
0.5	2.8912	17.9313	4.6296	15.6146	16.196	38.7432	138.8552	135.9916	144.3728
0.6	2.6726	16.5715	4.2768	14.4328	14.968	35.8146	128.2996	125.7581	133.4832
0.8	2.3475	14.5554	3.7562	12.6773	13.1472	31.4593	112.6865	110.4928	117.2772
1	2.1113	13.0916	3.379	11.4017	11.8248	28.2923	101.3623	99.1956	105.3884
1.5	1.7145	10.6302	2.7432	9.2586	9.6016	22.9755	82.2970	80.7394	85.7062
2	1.4628	9.0692	2.3404	7.8988	8.1912	19.6004	70.2118	68.8811	73.1170
3	1.1502	7.1316	1.8404	6.2114	6.4416	15.4138	55.2122	54.1738	57.5094
4	0.9592	5.9467	1.5346	5.1795	5.3712	12.8528	46.0387	45.1762	47.9578
5	0.8281	5.1344	1.3250	4.4719	4.6376	11.0971	39.7501	39.0038	41.4048
6	0.7322	4.5378	1.1712	3.9527	4.0984	9.8078	35.1317	34.4779	36.6004
8	0.5982	3.7099	0.9574	3.2311	3.3512	8.0186	28.7217	28.1812	29.9168
10	0.5094	3.1583	0.8150	2.7509	2.8528	6.8266	24.4509	23.9966	25.4746

Table 5
Whole-atom total Compton scattering cross-sections (b/atom) for the biological materials in the energy region from 0.005 to 10 MeV using the tabulated values of Storm and Israel (1970).

Energy (MeV)	H_2O	$C_6H_{11}NO$	C_2H_4	$C_5H_8O_2$	C_8H_8	$C_{16}H_{14}O_3$	$C_{55}H_{102}O_6$	$H_8O_{26}P_9Ca_6$	$[Ca_3(PO_4)_2]_3$ Ca $(OH)_2$
0.005	3.3500	22.7350	6.2400	19.2100	20.8400	47.6100	181.4000	123.3900	127.8300
0.006	3.7540	24.9070	6.7680	21.1460	22.6960	52.2780	197.7040	140.1060	145.4740
0.008	4.3040	27.6920	7.4280	23.6860	25.0560	58.3680	218.4540	165.4060	172.2640
0.010	4.6360	29.5480	7.8720	25.3640	26.7040	62.5320	232.3360	183.0840	190.8560
0.015	5.0880	32.1990	8.4960	27.7620	29.1120	68.6160	251.9880	210.9420	220.4380
0.020	5.3120	33.5560	8.8040	28.9980	30.3680	71.8240	261.8620	226.6480	237.5320
0.030	5.4740	34.4020	8.9680	29.8160	31.1360	73.9580	267.6240	240.7760	253.2640
0.040	5.4620	34.2560	8.9040	29.7280	31.0080	73.7940	266.1120	244.4680	257.6320
0.050	5.3880	33.6790	8.7360	29.2620	30.4720	72.6360	261.3880	243.9820	257.4380
0.060	5.3080	33.1340	8.5960	28.7820	29.9520	71.3960	257.1580	241.4920	255.0080
0.080	5.0720	31.5660	8.1640	27.4580	28.5280	68.1440	244.6220	233.8180	247.3120
0.100	4.8640	30.2120	7.8080	26.2960	27.2960	65.2480	234.0640	225.3260	238.5440
0.150	4.4060	27.3730	7.0720	23.8340	24.7440	59.1620	212.0560	205.6740	217.9860
0.200	4.0420	25.1060	6.4840	21.8580	22.6880	54.2540	194.4420	189.3480	200.8120
0.300	3.5260	21.8930	5.6520	19.0640	19.7840	47.3220	169.5260	165.5740	175.6460
0.400	3.1640	19.6270	5.0680	17.0960	17.7360	42.4280	152.0140	148.6860	157.7940
0.500	2.8880	17.8890	4.6160	15.5820	16.1520	38.6560	138.4880	135.8120	144.1580
0.600	2.6740	16.5470	4.2680	14.4160	14.9360	35.7580	128.0740	125.7560	133.4740
0.800	2.3500	14.5650	3.7600	12.6900	13.1600	31.4900	112.8000	110.5800	117.3700
1.000	2.1120	13.1110	3.3840	11.4180	11.8480	28.3440	101.5120	99.3880	105.5220
1.500	1.7140	10.6420	2.7480	9.2660	9.6160	22.9980	82.4140	80.7060	85.6840
2.000	1.4620	9.0640	2.3400	7.8980	8.1920	19.6020	70.2020	68.8780	73.1520
3.000	1.1510	7.1310	1.8400	6.2120	6.4400	15.4130	55.2060	54.2360	57.5560
4.000	0.9620	5.9610	1.5380	5.1930	5.3840	12.8860	46.1470	45.2680	48.0520
5.000	0.8310	5.1480	1.3280	4.4840	4.6480	11.1250	39.8460	39.1640	41.5560
6.000	0.7330	4.5500	1.1740	3.9630	4.1120	9.8390	35.2230	34.5660	36.7080
8.000	0.6000	3.7200	0.9600	3.2400	3.3600	8.0400	28.8000	28.2690	30.0060
10.000	0.5110	3.1700	0.8180	2.7610	2.8640	6.8530	24.5410	24.0650	25.5380

coefficients, up to few percent for low–z elements of dosimetric interest, in particular for molecular orbitals.

Various theoretical models for describing Compton scattering have been developed, to compare the energy and angular distribution of the scattered photons (Salvat and Fernandez-Varea, 2009; Salvat et al; Namito et al., 1994; Brown et al., 2014). Relativistic impulse approximation expression for Compton-scattering double differential cross sections and characterization of relativistic contributions at low-momentum- transfer non-relativistic limit was studied extensively and recovered the corresponding relativistic expression at low momentum transfer (LaJohn, 2010). There are major differences between the compared models especially at low photon energies. The small

Table 6
Whole-atom total Compton scattering cross-sections (b/atom) for the biological materials in the energy region from 0.005 to 10 MeV using XCOM (Berger and Hubbell, 1987).

Energy (MeV)	H_2O	$C_6H_{11}NO$	C_2H_4	$C_5H_8O_2$	C_8H_8	$C_{16}H_{14}O_3$	$C_{55}H_{102}O_6$	$H_8O_{26}P_9Ca_6$	$[Ca_3(PO_4)_2]_3$ Ca $(OH)_2$
0.005	3.3574	22.1577	6.0428	18.7156	20.0216	45.9748	175.9654	123.5216	127.8834
0.006	3.7606	24.4243	6.6052	20.7424	22.0184	50.9312	193.2306	140.2564	145.6006
0.008	4.3080	27.4030	7.3300	23.4350	24.6480	57.5450	215.7370	165.1980	172.0200
0.010	4.6386	29.3063	7.7912	25.1574	26.3704	61.8592	230.0976	182.7654	190.5346
0.015	5.0890	32.0895	8.4620	27.6640	28.9720	68.3170	251.0130	210.5860	220.0150
0.020	5.3136	33.5038	8.7912	28.9484	30.3104	71.6832	261.4556	226.3594	237.1536
0.030	5.4748	34.4024	8.9696	29.8112	31.1392	73.9516	267.6408	240.5822	253.0148
0.040	5.4618	34.2369	8.8956	29.7172	30.9752	73.7436	265.9118	244.4142	257.5378
0.050	5.3894	33.6977	8.7388	29.2776	30.4776	72.6608	261.4894	243.8926	257.3114
0.060	5.2888	33.0234	8.5536	28.7092	29.8592	71.2506	256.1108	241.3542	254.8828
0.080	5.0732	31.6016	8.1744	27.4908	28.5648	68.2284	244.9272	233.7948	247.2512
0.100	4.8646	30.2423	7.8172	26.3184	27.3304	65.3162	234.3146	225.3614	238.5546
0.150	4.4070	27.3665	7.0680	23.8250	24.7240	59.1240	211.9480	205.7190	218.0290
0.200	4.0428	25.1264	6.4876	21.8782	22.6992	54.2936	194.5738	189.5852	201.0448
0.300	3.5270	21.8875	5.6500	19.0600	19.7720	47.3000	169.4730	165.6460	175.7430
0.400	3.1636	19.6238	5.0652	17.0894	17.7264	42.4092	151.9386	148.7054	157.8016
0.500	2.8886	17.9273	4.6272	15.6134	16.1944	38.7462	138.8056	135.9564	144.2886
0.600	2.6752	16.5846	4.2804	14.4438	14.9808	35.8434	128.4042	125.8308	133.5552
0.800	2.3502	14.5711	3.7604	12.6908	13.1608	31.4914	112.8102	110.6168	117.4122
1.000	2.1128	13.1034	3.3816	11.4132	11.8352	28.3206	101.4488	99.5012	105.6168
1.500	1.7136	10.6518	2.7492	9.2774	9.6224	23.0232	82.4726	80.8804	85.8536
2.000	1.4632	9.2686	2.3454	7.9163	8.2088	19.6434	70.3637	69.0328	73.2792
3.000	1.1496	7.1502	1.8452	6.2276	6.4584	15.4540	55.3562	54.3160	57.6582
4.000	0.9634	5.9644	1.5392	5.1948	5.3872	12.8908	46.1760	45.3102	48.1000
5.000	0.8312	5.1512	1.3294	4.4865	4.6528	11.1332	39.8813	39.1244	41.5318
6.000	0.7338	4.5524	1.1748	3.9650	4.1120	9.8394	35.2442	34.5826	36.7152
8.000	0.6000	3.7234	0.9608	3.2430	3.3632	8.0479	28.8250	28.2871	30.0284
10.000	0.5112	3.1709	0.8182	2.7619	2.8640	6.8537	24.5475	24.0943	25.5778

Table 7
Compton energy absorption cross-sections (b/atom) for the biological materials in the energy region from 0.5 to 10 MeV using tabulated values of Biggs et al. (1975).

Energy (MeV)	H_2O	$C_6H_{11}NO$	C_2H_4	$C_5H_8O_2$	C_8H_8	$C_{16}H_{14}O_3$	$C_{55}H_{102}O_6$	$H_8O_{26}P_9$ Ca_6	$[Ca_3(PO_4)_2]_3$ Ca $(OH)_2$
0.005	0.0833	0.2658	0.0690	0.2317	0.2352	0.5643	2.0649	1.7452	1.7832
0.006	0.1033	0.3330	0.0870	0.2891	0.2960	0.7059	2.5943	2.1952	2.2542
0.008	0.1449	0.4687	0.1230	0.4059	0.4192	0.9951	3.6595	3.1456	3.2470
0.010	0.1874	0.6048	0.1588	0.5232	0.5432	1.2872	4.7226	4.0662	4.2268
0.015	0.2936	0.9406	0.2466	0.8137	0.8488	2.0106	7.3387	6.4202	6.7108
0.020	0.3947	1.2567	0.3286	1.0881	1.1352	2.6927	9.7915	8.6986	9.1150
0.030	0.5770	1.8237	0.4752	1.5812	1.6480	3.9174	14.1844	12.8871	13.5406
0.040	0.7331	2.3074	0.6000	2.0026	2.0848	4.9629	17.9290	16.5431	17.4038
0.050	0.8661	2.7200	0.7064	2.3620	2.4568	5.8537	21.1218	19.7182	20.7806
0.060	0.9798	3.0722	0.7972	2.6690	2.7744	6.6146	23.8474	22.4466	23.6792
0.080	1.1604	3.6311	0.9412	3.1562	3.2784	7.8224	28.1710	26.8095	28.3222
0.100	1.2929	4.0421	1.0472	3.5144	3.6488	8.7097	31.3522	30.0285	31.7514
0.150	1.4873	4.6449	1.2026	4.0397	4.1920	10.0111	36.0165	34.7798	36.8204
0.200	1.5680	4.8922	1.2660	4.2562	4.4144	10.5468	37.9262	36.7821	38.9626
0.300	1.5772	4.9204	1.2732	4.2806	4.4400	10.6080	38.1426	37.0967	39.3174
0.400	1.5121	4.7168	1.2204	4.1036	4.2560	10.1691	36.5624	35.6086	37.7486
0.500	1.4282	4.4543	1.1524	3.8754	4.0192	9.6038	34.5266	33.6527	35.6800
0.600	1.3336	4.1801	1.0840	3.6256	3.7808	9.0044	32.4180	31.4116	33.3218
0.800	1.1920	3.7176	0.9618	3.2345	3.3544	8.0154	28.8163	28.1115	29.8104
1.000	1.0678	3.3304	0.8616	2.8976	3.0048	7.1802	25.8144	25.1903	26.7128
1.500	0.8475	2.6431	0.6838	2.2997	2.3848	5.6987	20.4875	19.9981	21.2076
2.000	0.7049	2.1981	0.5686	1.9125	1.9832	4.7393	17.0367	16.6356	17.6428
3.000	0.5316	1.6581	0.4290	1.4427	1.4960	3.5748	12.8531	12.5483	13.3090
4.000	0.4290	1.3371	0.3458	1.1635	1.2064	2.8834	10.3623	10.1266	10.7404
5.000	0.3609	1.1250	0.2910	0.9789	1.0152	2.4261	8.7195	8.5188	9.0362
6.000	0.3120	0.9727	0.2516	0.8464	0.8776	2.0974	7.5390	7.3666	7.8134
8.000	0.1478	0.4722	0.1000	0.4218	0.2984	0.8672	3.2400	5.8188	6.1710
10.000	0.2042	0.6364	0.1646	0.5537	0.5744	1.3726	4.9321	4.8201	5.1132

difference between the values given by Ribberfors and the ones calculated here may be due to the different binding energies used, which affect the atomic cross section at low photon energies. The atomic cross section according to the incoherent scattering function approach deviate greatly from the relativistic impulse approximation at low energies. The differences are less than 0.3% in between 0.005 and 10 MeV.

The motion of the atomic electrons around the atomic nucleus gives rise to a Doppler broadening of the apparent energy of the incident photon, resulting in a corresponding broadening of the Compton "modified line" for a given deflection angle of the outgoing scattered photon. The shape of this broadened line is called the "Compton profile". Compton profiles J (p_z), calculated using Hartree-Fock wave functions are available in the literature (Biggs et al., 1975). Geometrical factor influence on Compton profile measurements for few biological materials

Table 8
Compton energy absorption cross-sections (b/atom) for the biological materials in the energy region from 000.5 to 10 MeV using tabulated values of Storm and Israel (1970).

Energy (MeV)	H_2O	$C_6H_{11}NO$	C_2H_4	$C_5H_8O_2$	C_8H_8	$C_{16}H_{14}O_3$	$C_{55}H_{102}O_6$	$H_8O_{26}P_9Ca_6$	$[Ca_3(PO_4)_2]_3$ Ca $(OH)_2$
0.005	0.0320	0.2173	0.0596	0.1836	0.1992	0.4552	1.7330	1.1810	1.2238
0.006	0.0431	0.2855	0.0776	0.2424	0.2600	0.5989	2.2666	1.6063	1.6676
0.008	0.0651	0.4190	0.1124	0.3584	0.3792	0.8833	3.3056	2.5033	2.6074
0.010	0.0869	0.5534	0.1474	0.4751	0.5000	1.1711	4.3509	3.4319	3.5776
0.015	0.1406	0.8900	0.2348	0.7674	0.8048	1.8970	6.9646	5.8384	6.1016
0.020	0.1918	1.2109	0.3176	1.0462	1.0952	2.5906	9.4468	8.1812	8.5718
0.030	0.2846	1.7918	0.4672	1.5524	1.6224	3.8522	13.9396	12.5214	13.1716
0.040	0.3638	2.2834	0.5936	1.9812	2.0672	4.9186	17.7388	16.2892	17.1668
0.050	0.4352	2.7161	0.7044	2.3608	2.4568	5.8584	21.0802	19.6958	20.7822
0.060	0.4960	3.0960	0.8020	2.6910	2.8000	6.6800	24.0110	22.6490	23.9240
0.080	0.5938	3.6954	0.9556	3.2142	3.3392	7.9766	28.6338	27.3462	28.9088
0.100	0.6708	4.1689	1.0776	3.6282	3.7672	9.0036	32.3008	31.1092	32.9498
0.150	0.7998	4.9684	1.2836	4.3262	4.4912	10.7386	38.4898	37.3872	39.6148
0.200	0.8736	5.4258	1.4012	4.7234	4.9024	11.7232	42.0186	40.9304	43.4236
0.300	0.9504	5.9052	1.5248	5.1416	5.3376	12.7648	45.7304	44.6416	47.3704
0.400	0.9806	6.0843	1.5712	5.2994	5.4984	13.1522	47.1256	46.1004	48.9006
0.500	0.9902	6.1331	1.5824	5.3418	5.5368	13.2514	47.4752	46.5248	49.3702
0.600	0.9816	6.0743	1.5672	5.2914	5.4824	13.1232	47.0216	46.1864	49.0266
0.800	0.9542	5.9256	1.5304	5.1608	5.3568	12.8114	45.8992	44.8728	47.6092
1.000	0.9256	5.7448	1.4832	5.0024	5.1904	12.4152	44.4856	43.4424	46.1056
1.500	0.8442	5.2421	1.3544	4.5638	4.7368	11.3254	40.6092	39.6248	42.0542
2.000	0.7728	4.7924	1.2376	4.1752	4.3312	10.3616	37.1228	36.2772	38.5228
3.000	0.6578	4.0794	1.0536	3.5512	3.6832	8.8086	31.5928	30.7142	32.5448
4.000	0.5764	3.5722	0.9228	3.1106	3.2256	7.7148	27.6714	26.7956	28.3764
5.000	0.5132	3.1891	0.8244	2.7748	2.8808	6.8844	24.7082	23.7948	25.1922
6.000	0.4632	2.8851	0.7464	2.5098	2.6088	6.2304	22.3632	21.3738	22.6182
8.000	0.3900	2.4270	0.6280	2.1100	2.1920	5.2340	18.8100	17.9350	18.9620
10.000	0.3390	2.1150	0.5480	1.8380	1.9120	4.5610	16.4040	15.4670	16.3180

Table 9
Compton component of mass energy absorption coefficients (cm^2/g) for few biological materials in the energy region from 0.005 to 10 MeV estimated using mixture rule.

Energy (MeV)	H_2O	$C_6H_{11}NO$	C_2H_4	$C_5H_8O_2$	C_8H_8	$C_{16}H_{14}O_3$	$C_{55}H_{102}O_6$	$H_8O_{26}P_9$ Ca_6	$[Ca_3(PO_4)_2]_3$ Ca $(OH)_2$
0.005	0.0015	0.0014	0.0015	0.0014	0.0013	0.0013	0.0014	0.0011	0.0011
0.006	0.0019	0.0018	0.0018	0.0017	0.0017	0.0017	0.0018	0.0014	0.0014
0.008	0.0026	0.0025	0.0027	0.0025	0.0024	0.0024	0.0026	0.0020	0.0020
0.010	0.0033	0.0032	0.0034	0.0031	0.0031	0.0030	0.0033	0.0026	0.0025
0.015	0.0051	0.0050	0.0053	0.0049	0.0049	0.0048	0.0052	0.0041	0.0040
0.020	0.0067	0.0067	0.0071	0.0066	0.0066	0.0064	0.0069	0.0056	0.0055
0.030	0.0098	0.0097	0.0102	0.0095	0.0095	0.0092	0.0099	0.0082	0.0081
0.040	0.0123	0.0123	0.0129	0.0120	0.0121	0.0118	0.0126	0.0105	0.0104
0.050	0.0146	0.0145	0.0152	0.0142	0.0142	0.0139	0.0148	0.0126	0.0125
0.060	0.0165	0.0164	0.0171	0.0161	0.0161	0.0157	0.0167	0.0143	0.0142
0.080	0.0195	0.0193	0.0202	0.0190	0.0190	0.0185	0.0197	0.0171	0.0170
0.100	0.0217	0.0215	0.0225	0.0211	0.0211	0.0206	0.0220	0.0192	0.0191
0.150	0.0251	0.0247	0.0258	0.0243	0.0242	0.0237	0.0252	0.0222	0.0221
0.200	0.0264	0.0260	0.0272	0.0256	0.0255	0.0250	0.0266	0.0235	0.0233
0.300	0.0265	0.0262	0.0273	0.0257	0.0256	0.0251	0.0267	0.0237	0.0235
0.400	0.0255	0.0251	0.0262	0.0247	0.0247	0.0241	0.0257	0.0227	0.0226
0.500	0.0240	0.0237	0.0247	0.0233	0.0232	0.0228	0.0242	0.0215	0.0214
0.600	0.0222	0.0222	0.0233	0.0218	0.0218	0.0213	0.0227	0.0200	0.0199
0.800	0.0200	0.0198	0.0206	0.0194	0.0194	0.0189	0.0202	0.0179	0.0179
1.000	0.0180	0.0178	0.0185	0.0175	0.0174	0.0170	0.0181	0.0161	0.0160
1.500	0.0143	0.0141	0.0147	0.0139	0.0138	0.0135	0.0144	0.0128	0.0127
2.000	0.0118	0.0117	0.0122	0.0115	0.0115	0.0112	0.0119	0.0106	0.0106
3.000	0.0089	0.0088	0.0092	0.0087	0.0087	0.0085	0.0090	0.0080	0.0080
4.000	0.0072	0.0072	0.0075	0.0070	0.0070	0.0069	0.0073	0.0065	0.0065
5.000	0.0060	0.0060	0.0062	0.0059	0.0058	0.0057	0.0061	0.0054	0.0054
6.000	0.0052	0.0052	0.0054	0.0051	0.0051	0.0050	0.0053	0.0047	0.0047
8.000	0.0041	0.0040	0.0038	0.0039	0.0036	0.0035	0.0035	0.0036	0.0036
10.000	0.0035	0.0034	0.0036	0.0034	0.0033	0.0033	0.0035	0.0031	0.0039

has been studied extensively (Brunetti et al., 2004). Recently, tomographic based scattered radiation from biological materials is examined using synchrotron X-rays. (Rao et al., 2005). In addition, synchrotron-based scattered radiation from low-contrast phantom materials form polyethylene (C_2H_4), polystyrene (C_8H_8), nylon ($C_6H_{11}NO$) and plexiglass ($C_{43}H_{38}O_7$), used as test objects in X-ray CT was examined with 8, 10 and 12 keV X-rays (Rao et al., 2009). These test phantom materials of medical interest will contains varying proportions of low atomic number elements. Based on the above theoretical and experimental evidence, the impact of the Compton profile on the computation of X-ray cross section and attenuation coefficients derived are very useful.

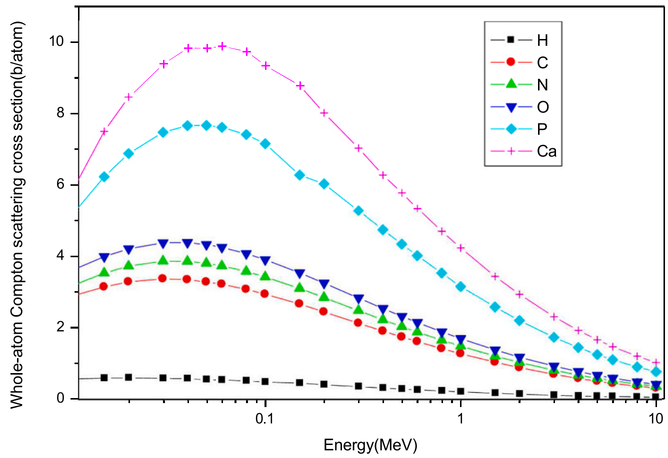

Fig. 1. Compton scattering cross-sections (b/atom) for H, C, N, O, P and Ca in the energy region 0.005–10 MeV, using the tabulated values of Biggs et al., (1975).

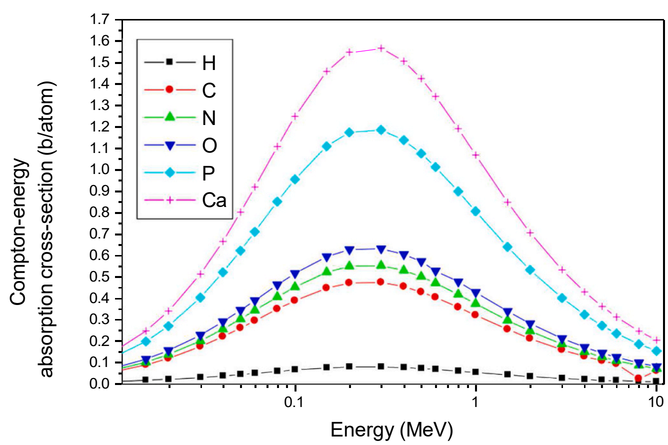

Fig. 2. Compton energy absorption cross-sections (b/atom) for H, C, N, O, P and Ca in the energy region
0.005–10 MeV, using the tabulated values of Biggs et al., (1975).

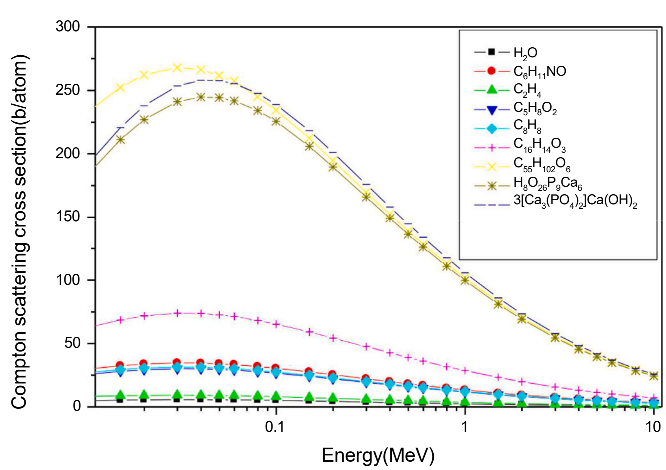

Fig. 3. Whole-atom total Compton scattering cross-sections (b/atom) for the biological materials in the energy region from 0.5 to 10 MeV using the tabulated values of Biggs et al., (1975).

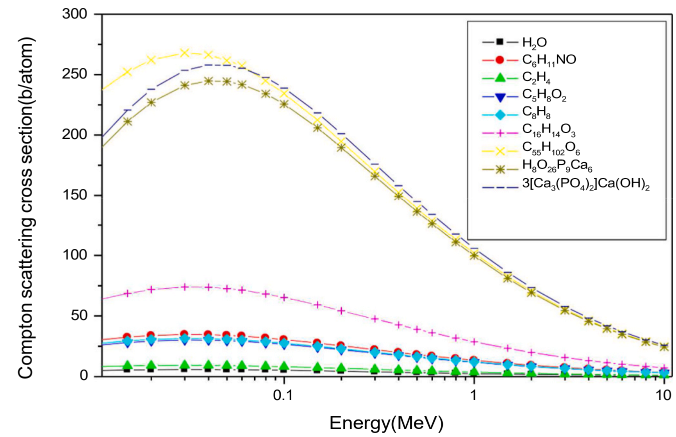

Fig. 4. Whole-atom total Compton scattering cross-sections (b/atom) for the biological materials in the energy region from 0.5 to 10 MeV using the tabulated values of Storm and Israel (1970).

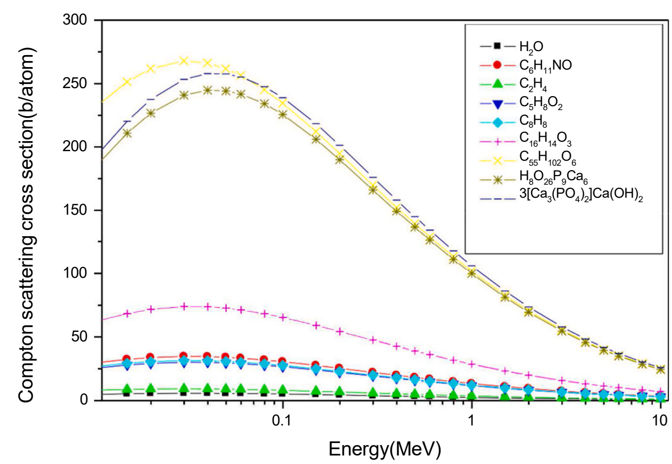

Fig. 5. Whole-atom total Compton scattering cross-sections (b/atom) for the biological materials in the energy region from 0.5 to 10 MeV using the tabulated values of XCOM (Berger and Hubbell 1987).

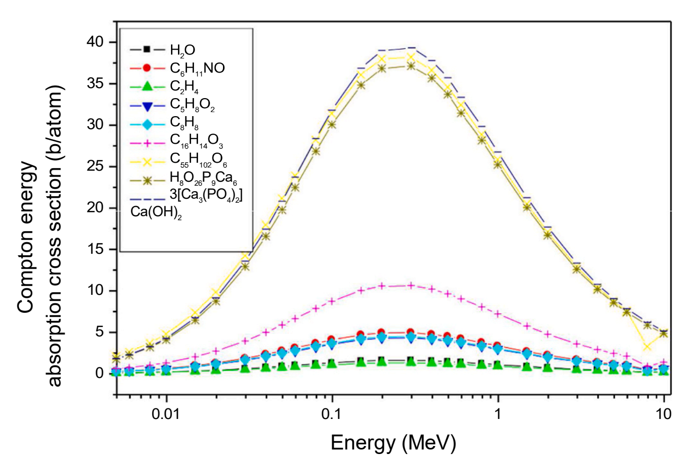

Fig. 6. Compton scattering energy absorption cross-sections (b/atom) for the biological materials in the energy region from 0.5 to 10 MeV using the tabulated values of Biggs et al., (1975).

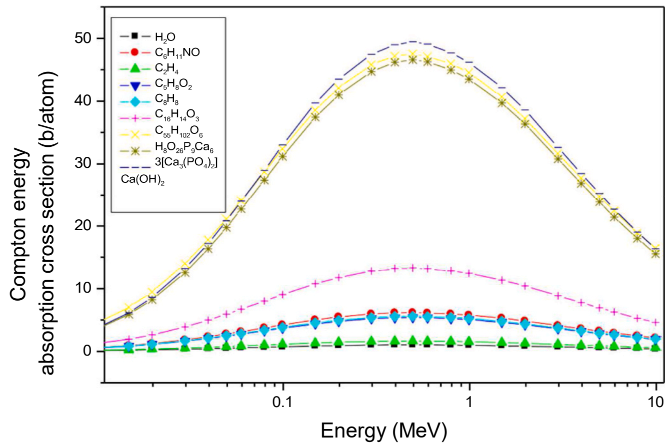

Fig. 7. Compton scattering energy absorption cross-sections (b/atom) for the biological materials in the energy region from 0.5 to 10 MeV using the tabulated values of Storm and Israel (1970).

2. Theoretical methods

Impulse approximation based double differential scattering cross sections for Compton scattering against bound electron states, effects of anisotropy and polarization, are studied extensively, with approximate relativistic treatment, valid for all scattering angles. A simple relationship between the cross section and the Compton profile is obtained (Ribberfors, 1975). It accounts for the Doppler broadening of the double differential cross section. It is defined as

$$J_i(p_z) = \iint \rho_i(p_e)\, dp_x\, dp_y \tag{1}$$

where ρ_i (p_e) = |ψ(p_e) |2 is the initial electron momentum distribution and ψ(p_e) is the electron wave function. Due to wave function normalization, Compton profiles are normalized to unity as

$$\int_{\infty}^{-\infty} J_i(p_z)\, dp_z = 1 \tag{2}$$

The Compton profile, J (p_Z), in eq's (1) and (2) takes into account the fact that the electrons in the atom has distribution of velocities. This causes a Doppler shift for the scattered photon. Instead of the single Compton energy, the scattered photons show a broadened spectrum of energies.

In the Hartree-Fock approximation, the electron momentum distribution is isotropic, and the Compton profile reduces

$$J_i(p_z) = 2\pi \int_{p_z}^{\infty} p\, \rho_i(p)\, dp \tag{3}$$

The relativistic double differential cross section for scattering of an initially unpolarised X-ray photon is as follows (Ribberfors and Berggren, 1982).

$$d^2\sigma \;/\; d\omega' d\Omega' = \left(r_0^2 / 2\right)\, m\, (\omega_2 / \omega_1)|k - k'|\, X_{KN}\, J(p_z) \tag{4}$$

The above expression is further simplified by putting $\omega_1 \approx \omega_2$ in X_{KN}. The non-relativistic expression in the above approximation is

$$d^2\sigma \;/\; d\omega' d\Omega' \ldots = \left(r_0^2 / 2\right)\, m\, (\omega_2 / \omega_1)|k - k'|\, \left(1 + \cos^2(\theta)\right) J(p_z), \textit{where}$$

$$|k - k'| = \left(\omega_1^2 + \omega_2^2 - 2\,\omega_1\,\omega_2 \cos(\theta)\right)^{0.5}$$
$$\textit{and}\ X_{KN} = \frac{\omega^1}{\omega_2^c} + \frac{\omega_2^c}{\omega_1} - \sin^2\theta \tag{5}$$

The numerical difference in using eq's (4) and (5) is of the order of less than 1% if integrated over the scattered photon energy.

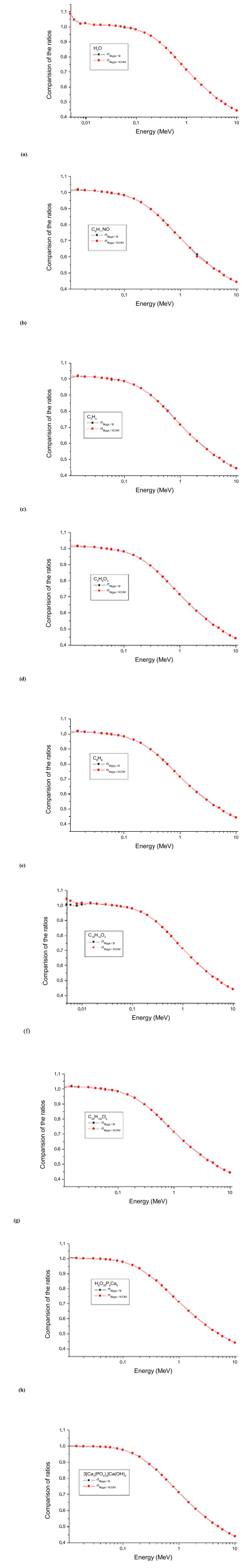

Fig. 8. (a)–(h). Comparison of the ratios in the energy region 0.005 to MeV (a) Water (b) Nylon(c) Polyethylene (d) Lucite (e) Polystyrene (f) Polycarbonate (g) Fat (h) Bone.(i) Calcium hydroxyapatite.

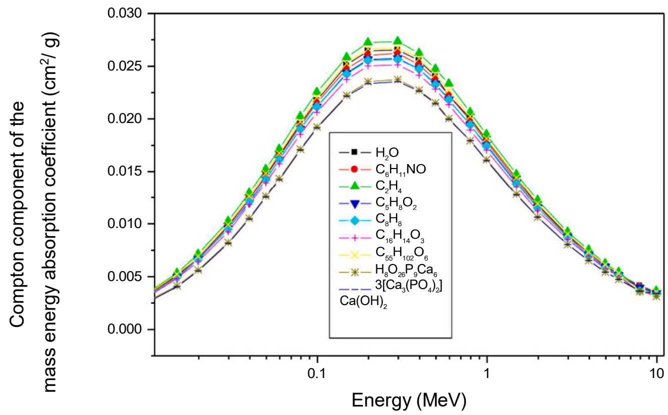

Fig. 9. Compton component of mass energy absorption coefficients (cm^2/g) for few biological materials in the energy region from 0.005 to 10 MeV estimated using mixture rule.

The total cross sections are calculated using linear approximations and the energy absorption cross section for electrons scattered by photons with the use of the same method. The approximate method requires the knowledge of the Ji (0)'s and the binding energies for the electrons. The most and commonly used Compton profiles are Hartree-Fock Compton profiles calculated by Biggs et al. (1975). The Compton profile can be interpreted as a probability density function of p_z. In the case of Hartree-Fock Compton profiles, J_i (p_z) is symmetric about $p_z = 0$ for all the shells of every element. Also, the maximum of J_i (p_z) is obtained at $p_z = 0$ for all the shells. In general, J_i (p_z) is broader for inner shells and becomes highly peaked at $p_z = 0$ as the shell number increases. Similar to Compton profiles, the double differential cross section is narrowly peaked at ωc and corresponding to $p_z = 0$. When considering the atomic double differential cross section, the most probable scattered photon energy is usually equal to ω_c.

The total cross section is obtained by integrating eq (4) over energy and solid angle intervals and the cross section for a specific shell (σ_i) is obtained.

$$\sigma_i = \left(m \pi r_0^2 / \omega_1\right) \iint d\theta \, d\omega_2 \left(\omega_2 \Big/ |k - k'| \left(\frac{\omega_1}{\omega_2^c} + \frac{\omega_2^c}{\omega_1} - \sin^2\theta \right) \sin\theta \, J_i(p_z) \right) \tag{6}$$

The limit of the integration in eq (6) for the energy of the scattered photon 'ω_2' up to 'ω_2' = ω_1 – i where 'i' is the ionization energy of the electron in the 'i' th shell and 'ω_2^c' is the energy of the Compton scattered photon. The total cross section is the summation over the occupied shells. It can be written as follows (Ribberfors, 1983).

$$\sigma_i = \pi r_0^2 \int_0^\pi d\theta \left(\frac{\omega_2^c}{\omega_1}\right)^2 \left(\frac{\omega_1}{\omega_2^c} + \frac{\omega_2^c}{\omega_1} - \sin^2\theta\right) \sin\theta \int_{-m}^{p_{\max}} dp_z \, J_i(p_z) \tag{7}$$

Further approximations are as follows

$$P_z = \omega_1\omega_2(1 - \cos\theta) - m(\omega_1 - \omega_2)\left[\left(\omega_1^2 + \omega_2^2 - 2\,\omega_1\omega_2(1 - \cos\theta)\right)^{0.5}\right]^{-1}$$

$$d\omega_2 \Big/ dp_z = |k - k'|\left[m\left(\frac{\omega_1}{\omega_2}\right)\right] - p_z(\omega_2 - \omega_1 \cos\theta) \Big/ |k - k'|^{-1} \tag{8}$$

With the use of eq' (7) and (8), the following equation has been derived for energy absorption cross section.

$$\sigma_{en} = \pi r_0^2 \int_0^\pi d\theta \sin\theta \left(\frac{\omega_2^c}{\omega_1}\right)\left(1 - \frac{\omega_2^c}{\omega_1}\right)\left\{\frac{\omega_1}{\omega_2^c} + \frac{\omega_2^c}{\omega_1} - \sin^2\theta\right\} X \sum \int_{-m}^{p_{\omega_1 - I_i}} dp_z \; J_i(p_z)\left\{1 + \alpha(\omega_1, \omega_2^c, \theta) p_z \big/ m + \beta\left((\omega_1, \omega_2^c, \theta)(p_Z/m^2)\right)\right\}(1 - g(Z)) \tag{9}$$

where 'r_o' is the classical electron radius, 'm' is the electron mass, ω_1 and ω_2^c are the incident and scattered photon energies for an electron at rest in keV, 'θ' is the scattering angle and J_i (p_z) is the Compton profile of an electron in the i th shell. In eq's (7) and (9) 'P_{imax}' is the highest 'P_z' value for which an electron in orbital number 'i' is able to be excited. The 'P_{imax}' is obtained by putting 'ω_2^c' up to 'ω_2^c' = ω_1 – i, in eq (7), where 'i' is the ionization energy of the electron in the 'i' th shell. The 'P_{imax}' may be positive or negative.

The values for 'α' and 'β' are obtained with the use of series expansion. With this procedure, the first term in eq. (9) becomes normalization integral for Compton profile number 'i'. The summation over 'i' gives the atomic number 'Z' for the material. The second term is zero, since the integrand is an odd function of p_z. is in first order. The third term may be neglected, or used as a correction, because it is of second order $(p_z/m)^2$. The integration is over the solid angle d Ω′ and the energy integration is extended to all the shells K, L, M. for electrons in the orbits. In eq (9) g (ω_1- ω_2, Z) is the expectation value of the fraction of the energy transfer (ω_1- ω_2) which is lost due to bremsstrahlung when the liberated secondary electrons (the Compton electron, Auger and Coster - Kronig electrons) are slowed down.

The Compton profile data introduces some difficulties about the appropriate interpolation and extrapolation techniques. First of all, the tabulated Compton profiles do not cover the whole range of p_z because p_z min/($\alpha m_e c$) ≈ −137. Also, the maximum value of $p_z/(\alpha m_e c)$ can be much larger than 100. It is observed for outer shells for which the Compton profiles are highly peaked at $p_z = 0$. However, inner shells have much broader distributions, indicates that p_z grid of the profile data is not sufficient and the Compton profiles must be extrapolated above $p_z/(\alpha m_e c) = 100$. Another issue is the proper interpolation of the Compton profiles, which again a real problem for broader profiles. Linear interpolation is sufficient for outer shells, because most of the Compton profile data are given at small values of p_z. For the broad inner-shell profiles roughly above $p_z/(\alpha m_e c) = 30$, linear interpolation is not sufficient as it causes artifacts in double differential cross section. Useful interpolation and extrapolation methods for the Compton profile data are not available in the literature. The validity of interpolation and extrapolation schemes uses the normalization condition of eq. (3), tighter with graphical analysis. Linear interpolation and extrapolation on a log-liner scale proved to be reasonably good approximations. With the present procedure, the earlier, anomalies and discrepancies are corrected.

The whole atom scattering cross section for unpolarised photons for each subshell is evaluated using the following relation

$$d^2\sigma \Big/ d\omega' d\Omega' = \sum N_i \left(d^2\sigma \big/ d\omega' d\Omega'\right)_i J_i(p_z) \tag{10}$$

here 'i' denotes the sub-shell number, 'N_i' is the number of electrons in the 'i' th shell and J_i (p_Z) is the Compton profile of an electron in the 'i' th shell. However, the summation exclude those electrons for which (ω_1- ω_2) < E_B. Energy transfers (ω_1- ω_2) less than the binding energy of the electrons cannot occur. The presence of the absorption edge causes a considerable asymmetry in the energy distribution of the Compton scattered photons, particularly at low incident photon energies.

The Compton profile for the molecules, plastics and tissues is calculated by weighted addition, e.g., for bone,

$$J_i(p_z) = 8J(p_z)_H + 26J(p_z)_o + 9J(p_z)_p + 6J(p_z)_{Ca} \tag{11}$$

Our calculations are based on the following approximations and easy to evaluate the total scattering cross-sections and Compton energy absorption cross-sections for the individual shells and the whole-atom. We adopted the following procedure for the limits of integration: ω_2 (max) = ω_1 - ω_2, $E_{KE} = \omega_1 - \omega_2 - E_B$, $\omega_2 = \omega_2$ (max), $\omega_2 = \omega_2$ (max)/2000 values for the scattered photon energy. The numerical integration analysis is performed using the C++ computer program. We generated the Compton profile function with the use of J_i (0)'s and the binding energies for the electrons. For each incoming photon energy, we have entered the number of shells/sub-shells in atom manually.

This program generates the data with exclusion of those electrons for which ω_1- ω_2 < E_B in eq (9) by introducing an absorption edge in the double differential cross section. In this way we entered the binding energy for each shell and also with exclusion of those electrons for which ω_1- ω_2 < E_B and the data is evaluated in the energy region from 0.005 to 0.5 MeV. The computer program evaluates the data required for the study (DDCS Single shell, DDCS all shells, DCS single shell, DCS all shells, Compton profile single shell, Compton profile all shells, S (X,Z) single value and S (X,Z)/Z multiple values).

3. Results and discussion

The, name, density and chemical formula of all the materials are presented in Table 1. Double differential scattering cross sections for single atoms such as, H, C, N, O, P and Ca are evaluated with eq's. (4) and (5) using the tabulated data of J_i (p_z). The difference between the two sets of derived relativistic and non-relativistic cross section is less than 1%. The numerical calculations are confined to the whole atom, based on impulse approximation. Whole-atom Compton scattering cross-sections (b/atom) for H, C, N, O, P, and Ca, and Compton-energy absorption cross sections in the energy region from 0.005 to 10 MeV using the tabulated Compton profile values of Biggs are presented in Tables 2 and 3.

Whole-atom total Compton scattering cross-sections for the biological materials in the energy region from 0.005 to 10 MeV using the Compton profile values of Biggs et al. (1975), Storm and Israel (1970), and using the XCOM, 1987, programme are presented in Table 4–6. Compton energy absorption cross-sections for the biological materials in the energy region from 0.005 to 10 MeV using tabulated values are presented in Tables 7 and 8. Compton component of mass energy absorption coefficients (cm^2/g) for few biological materials in the energy region from 0.005 to 10 MeV, estimated using mixture rule are presented in Table 9. The whole-atom Compton scattering cross-section and the Compton energy absorption cross sections for H, C., N, O, P and Ca are displayed in Figs. 1 and 2. The derived results for the biological materials using the tabulates values are displayed in Figs. 3–5 (Biggs et al., 1975; Storm and Israel., 1970; Berger and Hubbell, 1987). Compton energy absorption cross section evaluated using the tabulations of Biggs et al. (1975); Storm and Israel (1970), are presented in Figs. 6 and 7. The error arises due to the contribution of Doppler broadening from the individual shells. With inclusion of energy broadening of Compton scattered photons, reflects the true energy transferred to the Compton electrons. Comparison of the ratios for all the biological materials are displayed in Fig. 8. (a) to (i). The overall ratio for all the materials never exceeds more than 1.15, for all the biologically interesting elements. It is interesting to note that the energy absorption cross sections are less affected by the energy broadening of the Compton scattered photons. The Compton component of the absorption coefficients for the present materials in the energy region 0.005–10 MeV are displayed in Fig. (9). The values derived consistently follow the standard tabulations within the limited errors.

4. Conclusion

The results for the present biological materials are derived using the double differential cross section based on impulse approximation and highlighting the importance of Doppler broadening. In view of this, these values are useful in calculating the radiation attenuation, transport and energy deposition in medical physics, reactor shielding and industrial radiography.

CRediT authorship contribution statement

V Rao Donepudi: Methodology, Investigation. **E Gigante Giovanni:** Funding acquisition. **Tetsuya Yusa:** Investigation. **Tako Akatsuka:** Formal analysis. **Tohoru Takeda:** Funding acquisition. **Roberto Cesareo:** Project administration. **Antonio Brunetti:** Formal analysis. **Nick Schiavon:** Formal analysis.

Declaration of competing interest

The authors declare that they have no known competing financial interests or personal relationships that could have appeared to influence the work reported in this paper.

Data availability

Data will be made available on request.

Acknowledgements:

One of us (DVR) undertook part of this with a financial support from ICTP, Trieste, Italy. Continued the research as visiting professor, at Science Based Applications to Engineering, Physics Division, Universita di Roma “La Sapienza”, Via Scarpa 10, 00161, Roma, Italy, Istituto di Matematica e Fisica, Universita di Sassari, Italy and Department of Bio-Systems Engineering, Yamagata University, Yonezawa, Japan. I would be very grateful to Prof. Dr. Daniele Treleani, Head of the ICTP Programme for Training and Research in Italian Laboratories for continuous encouragement throughout the study.

References

Berger, M.J., Hubbell, J.H., 1987. XCOM: photon cross sections on a personal computer. NBSIR 87–3597.
Biggs, F., Mendelshon, L.B., Mann, J.B., 1975. Hartree-Fock Compton profiles for the elements. Atomic Data Nucl. Data Tables 16, 201–309.
Boone, J.M., Chavez, A.E., 1996. Comparison of x-ray cross sections for diagnostic and therapeutic medical physics. Med. Phy. 23, 1997–2005.
Brown, J., Dimmock, M., Gillan, J., Paganin, D., 2014. A low energy bound atomic electron Compton scattering model for Geant 4. Nucl. Instrum. Methods A 338, 77–88.
Brunetti, A., Cesareo, R., Rao, D.V., Golosio, B., 2004. Geometrical factor influence on Compton profile measurement for biological samples. Nucl. Instrum. Methods A 526, 584–592.
Brusa, D., Stutz, G., Riveros, J., Fernndez-Varea, J., Salvat, F., 1996. Fast sampling algorithm for the simulation of photon Compton scattering. Nucl. Instrum. Methods A 379, 167–175.
Carlsson, G.A., Carlsson, C.A., Berggren, K.-F., Ribberfors, R., 1982. Calculation of scattering cross sections for increased accuracy in diagnostic radiology. I. Energy broadening of Compton-scattered photons. Med. Phys. 9, 868–879.
Cesareo, R., Hanson, A.L., Gigante, G.E., Pedraza, L.J., Mahtaboally, S.Q.G., 1992. Interaction of keV photons with matter and new applications. Phys. Rep. 213, 117–178.
Cooper, M.J., 1985. Compton scattering and electron-momentum determination. Rep. Prog. Phys. 48, 415–481.
Grodstein, G.W., 1957. X-ray attenuation coefficients from 10 keV to 100 MeV. NBS Circular 583, 1–54.
Hubbell, J.H., 1977. Photon mass attenuation and mass energy-absorption coefficients for H, C, N, O, Ar, and seven mixtures from 0.1 keV to 20 MeV. Radiat. Res. 70, 58–81.
Hubbell, J.H., 1982. Photon mass attenuation and energy-absorption coefficients from 1 KeV to 20 MeV. Int. J. Appl. Radiat. Isot. 33, 1269–1290.
Hubbell, J.H., 1999. Review of photon interaction cross section data in the medical and biological context. Phys. Med. Biol. 44, R1–R22.
Hubbell, J.H., 2006. Review and history of photon cross section calculations. Phys. Med. Biol. 51, 245–262.
Hubbell, J.H., Veigele, W.J., Briggs, E.A., Brown, R.T., Cromer, D.T., Howerton, R.J., 1975. Atomic form factors, incoherent scattering functions, and photon scattering cross-sections. J. Phys. Chem. Ref. Data 4, 471–538.
Kane, P.P., 1997. Experimental studies of inelastic x-ray and γ-ray scattering. Radiat. Phys. Chem. 50, 31–62.
Kane, P.P., 2006. Inelastic scattering of X-rays and gamma rays. Radiat. Phys. Chem. 75, 2195–2205.
LaJohn, L.A., 2010. Low-momentum-transfer nonrelativistic limit of the relativistic impulse approximation expression for Compton scattering doubly differential cross section and characterization of their relativistic contributions. Phy.Rev.A. 81, 043404, 1 to 043404-13.
Namito, Y., Ban, S., Hirayama, H., 1994. Implementation of Doppler broadening of a Compton-scattered photon into the EGS4 code. Nucl. Instrum. Methods A 349, 489–494.

Rao, D.V., 2000. Doppler Broadening Calculations of Compton Scattering. Invited Talk. NIST, Gaithersburg, MD,USA.

Rao, D.V., Cesareo, R., Gigante, G.E., 1999. Whole-atom Compton scattering have unpolarised X-ray photons in the energy region 17.44 E 39.91 keV. Appl. Radiat. Isot. 50, 325–329.

Rao, D.V., Takeda, T., Itai, Y., Akatsuka, T., Cesareo, R., Brunetti, A., Gigante, G.E., 2002a. X-ray scattering cross-sections for molecules, plastics, tissues and few biological materials. J T M T 20, 327–361.

Rao, D.V., Takeda, T., Itai, Y., Akatsuka, T., Cesareo, R., Brunetti, A., Gigante, G.E., 2002b. Doppler broadening and its contribution to Compton energy-absorption cross-sections: an analysis of the Compton component in terms of mass-energy absorption coefficient. J. Phys. Chem. Ref. Data 31, 769–818.

Rao, D.V., Cesareo, R., Brunetti, A., Gigante, G.E., 2003. Compton energy absorption cross sections for H, C, N, O, P, Ca and assessment of Doppler broadening. Eur. Phys. J. D 23, 43–49.

Rao, D.V., Seltzer, S.M., Bergstrom, P.M., 2004a. Compton scattering cross-sections for individual shells for a few elements of biological interest in the energy region 5 keV-10 MeV. Radiat. Phys. Chem. 70, 479–489.

Rao, D.V., Cesareo, R., Brunetti, A., Gigante, G.E., Takeda, T., Itai, Y., Akatsuka, T., 2004b. Doppler broadening calculations of Compton scattering for molecules, plastics, tissues and few biological materials in the X-ray region: an analysis in terms of Compton broadening and geometrical energy broadening. J. Phys. Chem. Ref. Data 33, 627–712.

Rao, D.V., Yuasa, T., Akatsuka, T., Tromba, G., Hasan, M.Z., Takeda, T., 2005. Tomographic imaging based on scattered radiation from polyethylene using 10, 15, 20, 25 and 30 keV synchrotron X-rays with simple approximations. Nucl. Instrum. Methods B 239, 209–216.

Rao, D.V., Cesareo, R., Brunetti, A., Gigante, G.E., Takeda, T., Itai, Y., Akatsuka, T., 2007. NIM B. Whole-atom Compton scattering cross-sections and individual shell cross-sections for the biological elements in the energy region from 1 to 4 keV. NIMB 261, 193–196.

Rao, D.V., Swapna, M., Cesareo, R., Brunetti, A., Akatsuka, T., Yuasa, T., Takeda, T., Gigante, G.E., 2009. Synchrotron-based scattered radiation from phnatom materials used in X-ray CT. J. X Ray Sci. Technol. 18, 327–337.

Ribberfors, R., 1975. Relationship of the relativistic Compton cross section to the momentum distribution of bound electron states. Phy. Rev. B. 12, 2067–2074.

Ribberfors, R., 1983. X-ray incoherent scattering total cross sections and energy-absorption cross sections by means of simple calculation routines. Phys. Rev. A. 27, 3061–3070.

Ribberfors, R., Berggren, K.-F., 1982. Incoherent –x-ray scattering functions and cross-sections (dσ/dΩ')incoh by means of a pocket calculator. Phys. Rev. A. 26, 3325–3333.

Ribberfors, R., Carlsson, G.A., 1985. Compton component of the mass-energy absorption coefficient: corrections due to the energy broadening of Compton-scattered photons. Radiat. Res. 101, 47–59.

Salvat, F., Fernandez-Varea, J.M., 2009. Overview of physical interaction models for photon and electron transport used in Monte Carlo codes. Metrologia 46, S112–S138.

Salvat, F., Fernandez-Varea, J.M., Sempati, J., PENELOPE-2011. A Code System for Monte Carlo Simulation of Electron and Photon Transport. OECD-NEA, Issy-les-Moulineaux, France.

Seltzer, S.M., 1993. Calculation of photon mass energy-transfer and mass energy-absorption coefficients. Radiat. Res. 136, 147–170.

Storm, E., Israel, I., 1970. Photon cross sections from 1 keV to 100 MeV for elements **Z**= 1 to z=100. Nucl. Data Tables A. 7, 565–681.

Stutz, G., 2014. Compton-scattering cross-section for inner-shell electrons in the relativistic impulse approximation. Nucl. Instrum. Methods B 319, 8–16.

Wang, J.X., Miguel, B., Seuntjens, J., Fernández-Varea, J.M., 2020. On the relativistic impulse approximation for the calculation of Compton scattering cross sections and photon interaction coefficients used in kV dosimetry. Phy.Med.Biol. 65, 125010.